Int. J. Heat Mass Transfer. Vol. 34, No. 4/5, pp. 973–982, 1991
Printed in Great Britain

0017–9310/91 $3.00+0.00

Double wake flow with heat transfer

C. BEGUIER and P. FRAUNIE
Institut de Mécanique Statistique de la Turbulence, Unité Mixte No. 380033 Université/CNRS, 12 Avenue du Général Leclerc, 13003 Marseille, France

(*Received* 11 *January* 1990 *and in final form* 6 *June* 1990)

Abstract—This study concerns the dynamical and thermal fields downstream of a couple of cylinders. Different configurations are studied: cylinders with identical or different diameters, one being heated or not and the initial gap being variable. Firstly, parameters of similitude of the double wake flow are determined from the single cylinder wake laws, assuming a weak initial interaction and the linearization of the problem. From the definition of an equivalent diameter and an asymmetry coefficient, we are able to calculate the evolutions of the maximum velocity defect and of the mixing wake width. This analysis can be extended to the mixing of two plane perturbations such as the mixing of two plane jets in a uniform stream. Secondly the experimental part of the study presents measurements from hot-wire and visualizations in a hydrodynamical tunnel. The data concerning the mean dynamical field fit rather well the theoretical predictions in the similitude zone. Turbulent field measurements of the double and triple correlations between velocity and temperature fluctuations show the existence, in the asymmetrical case, of counter-gradient diffusions. These fluxes can be related to the largest eddies of the flow which create an important lateral diffusion from the small to the large cylinder.

1. INTRODUCTION

THIS EXPERIMENTAL study was realized in the complex turbulent shear flows domain presenting asymmetrical initial conditions for which two subjects of interest exist. Firstly, in this kind of flow, it is well known [1–3] that counter-gradient diffusions can appear, their study is important to define models of turbulence including the effect of the large structures of the flow [4]. Secondly the asymmetrical turbulent flows are in continuous rearrangement; for this reason they present interesting features from a theoretical point of view.

One of these flows concerns the double wake mixing behind two cylinders with equal or different diameters.

Zdravkovich [5] has given a general review of the literature concerning the wake of a twin cylinder with constant diameter and variable gap spacing.

The evolutions of the drag coefficient and of the Strouhal number have been measured by Bearman and Wadcock [6].

Below a critical gap, mixing is unstable with two different values for the drag. Landweber [7] detected the existence of a single vortex street for $e/\phi = 1$–1.25 and of two vortex streets for $e/\phi > 1.5$. This last author also noted a configuration with four vortex streets. Spivack [8] performed measurements of the vortex shedding by hot-wire anemometry in the range of Reynolds numbers $Re = 1.5\times10^4$–9.3×10^4. For small gap spacings, two frequencies can be measured: the highest corresponds to the Strouhal frequency of a single cylinder, the lowest can be associated to the couple of cylinders with a zero gap spacing. The flow is unstable with two solutions corresponding to an asymmetrical disposition of the Bénard–von Kármán vortex shedding with one more important street. The oscillation between the two solutions seems to occur randomly [9]. This asymmetrical configuration can be found back in the double wake flow with cylinders of different diameters. In a previous study published by Palmer and Keffer [10] the presence of a counter-gradient diffusion for the dynamic field has been noted from hot-wire measurements. To look in more detail at what is happening in this case, we performed an experimental network of the asymmetrical double wake flow by heating the small cylinder to include the diffusion of a scalar field. In our case, the temperature can be considered as a passive contaminant owing to the small Richardson numbers. So, we studied the dynamical turbulent field by different techniques: the hot-wire anemothermometry in an aerodynamic channel, one of the two cylinders being heated, and the laser-Doppler anemometry associated with visualizations in a water channel, with dye emission as a passive scalar contaminant.

To distinguish a double wake flow with equal or different diameters, with or without a heated cylinder we adopt the following nomenclature: the symmetrical case will be called $S_{i,j}$ and the asymmetrical case $A_{i,j}$. The first subscript represents the number of cylinders, the second one the number of heated cylinders. Sometimes, this indication will be followed by three numbers in parentheses (ϕ_1, L_0, ϕ_2) giving in millimetres the diameter of the small cylinder, the distance between the axes of the two cylinders and the diameter of the large cylinder.

2. SELF PRESERVATION PARAMETERS OF THE DOUBLE WAKE FLOW

2.1. *Single wake laws*

To study the mixing of the two cylinder wakes, it is interesting to define the self preserving parameters of

NOMENCLATURE

$A_{i,j}$ asymmetrical coupling of i cylinders, j being heated
a, b, c, d dynamic wake coefficients
C_p calorific capacity
C_x drag coefficient
H cylinder length
L_0 distance between the axes of two cylinders
$L(x)$ dynamic double wake width
L_θ thermal double wake width
l dynamic single wake width
l_θ thermal wake width
$(0, x, y)$ mean section of the mixing
q turbulent kinetic energy
q_0 initial heat flux
r diameter ratio, ϕ_1/ϕ_2
Re Reynolds number
S Strouhal number
$S_{i,j}$ symmetrical coupling of i cylinders, j being heated
U_e upstream velocity
$\Delta U_{\mathfrak{C}}$ centre-line velocity defect
x^* adimensional downstream distance of the double wake flow, $x\tilde{\phi}/L_0^2$.

Greek symbols
α interaction drag coefficient, $C_{x(1+2)}/C_{x_1}+C_{x_2}$
β asymmetry parameter
γ intermittency factor
ε_t eddy viscosity
η_u dynamic field similitude parameter, $(y-y_{U_{\min}})/L(x)$
η_θ thermal field similitude parameter, $(y-y_{\Theta_{\max}})/L_\theta(x)$
$\Delta\bar{\Theta}$ absolute temperature [K]
$\Delta\Theta_M$ maximum temperature excess
$\Delta\Theta_0$ initial overheat
ν kinematic viscosity
π turbulent production
ρ density
Φ cylinder diameter
$\tilde{\Phi}$ equivalent diameter of the double wake, $(\sqrt{\phi_1}+\sqrt{\phi_2})^2$.

Subscripts
$\mathfrak{C}$ centre-line value
u relative to the dynamic field
θ relative to the thermal field.

Superscripts
$\bar{}$ mean time value
$'$ fluctuation component.

the far field where we can consider the turbulent flow is established at first approximation.

A schematic diagram of the flow is presented on Fig. 1. The two axes of the cylinders are parallel and their plane is perpendicular to the upstream velocity U_e. The flow is considered as incompressible in the turbulent regime and two-dimensional in mean.

In the mixing of the two wakes, and for a given initial spacing gap L_0 between the two axes, it is possible to identify three downstream regions.

Firstly, just behind the cylinders the two wakes are developing more or less independently, the interaction

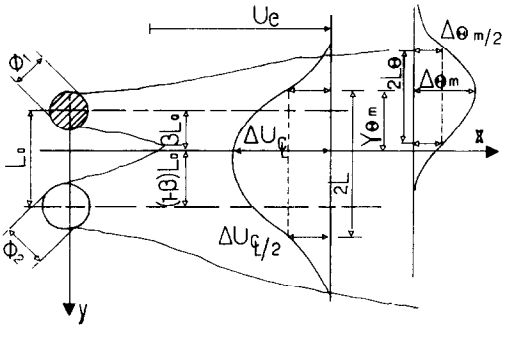

FIG. 1. Schematic diagram of the flow in the $A_{2,1}$ case.

mean effects will be characterized by the coupling coefficient α.

Secondly, there is a region where the mixing is evolving from the meeting point, located in the internal zone, to a downstream section far away, from which we can consider that the mixing is completely effective. This last section is the beginning of the third zone, characterized by the quasi self preservation of the velocity profiles, and it presents the same behaviour as a classical turbulent wake, driven by the approximated equations of motion, enthalpy and continuity, i.e.

$$U_e(\beta\Delta\bar{u}/\delta x)-(\delta/\delta y)(-\overline{u'v'})=0$$

$$U_e(\delta\Delta\bar{\Theta}/\delta x)-(\delta/\delta y)(-\overline{v'\theta'})=0$$

$$(\delta\Delta\bar{u}/\delta x)=(\delta\bar{v}/\delta y) \qquad (1)$$

where $\Delta\bar{u}=U_e-\bar{U}$ is the mean velocity defect in the downstream direction $0x$ and $\Delta\bar{\Theta}$ the mean overheat; u', v' and θ' are respectively the turbulent fluctuations of the velocity, in the $(0x, 0y)$ plane, and of the temperature. The self preservation conditions of the mean dynamic field can be expressed by

$$\Delta\bar{u}/\Delta U_{\mathfrak{C}}(x)=f(\eta) \quad \text{with} \quad \eta=y/L(x)$$

where $L(x)$ and $\Delta U_{\mathfrak{C}}(x)$ are the conventional length

and velocity scales. Assuming a Boussinesq closure model for the Reynolds stresses as

$$-\overline{u'v'} = \varepsilon_t \cdot \gamma[\delta(\Delta\bar{u}/\gamma)/\delta y] \tag{2}$$

where ε_t is the eddy viscosity and γ the intermittency factor varying [11] as

$$\gamma = [1+(\eta/\eta_0)^4]^{-1}$$

we obtain the following solution:

$$f(\eta) = \exp[-a\eta^2(1+d\eta^4)] \tag{3}$$

where a and d are constants, which can be experimentally determined. To complete the determination of the wake it is necessary to introduce two other constants, b and c, to describe the evolution of the maximum velocity defect and the wake width vs the downstream distance x/ϕ

$$\Delta U_{\mathfrak{C}}/U_e = b(x/\phi)^{-1/2}$$
$$L/\phi = (cx/\phi)^{1/2}. \tag{4}$$

From different data in the literature we shall adopt the following different values [12, 13]:

$$a = 0.6619;\ b = 1.066;\ c = 0.0745;\ d = 0.04695. \tag{5}$$

By analogy to the mean dynamic field, it is possible to obtain an asymptotic solution for the mean temperature, when considered as a scalar field. Because there is the same intermittency factor for the dynamic and the thermal fields in the wake of a heated cylinder, we shall write

$$\Delta\bar{\Theta}/\Delta\Theta_M = g(\eta_\theta) \quad \text{with} \quad \eta_\theta = y/L_\theta$$
$$g(\eta_\theta) = \exp -[a_\theta\eta_\theta^2(1+d_\theta\eta_\theta^4)] \tag{6}$$

and

$$\Delta\Theta_M/\Delta\Theta_0 = b_0(x/\phi)^{-1/2}$$
$$L_\theta/\phi = (c_\theta x/\phi)^{1/2} \tag{7}$$

where $\Delta\Theta_0 = q_0\pi/\rho C_p U_e$ is the initial overheat, q_0 being the heat flux at the cylinder surface. From different data in the literature [12, 13], we chose the following values for the different constants of the mean thermal field:

$$a_\theta = 0.533;\ b_\theta = 1.452;\ c_\theta = 0.142;\ d_\theta = 0.300. \tag{8}$$

It is interesting to remark about the constants given above for the dynamic wake of a cylinder.

For $y = L/2$ we obtain $\exp -a(1+d) = 1/2$ that is $a(1+d) = \ln 2 = 0.6931$.

In fact with the constants given by equation (5) we obtain $a(1+d) = 0.6930$.

On the other hand, the drag coefficient C_x can be written as

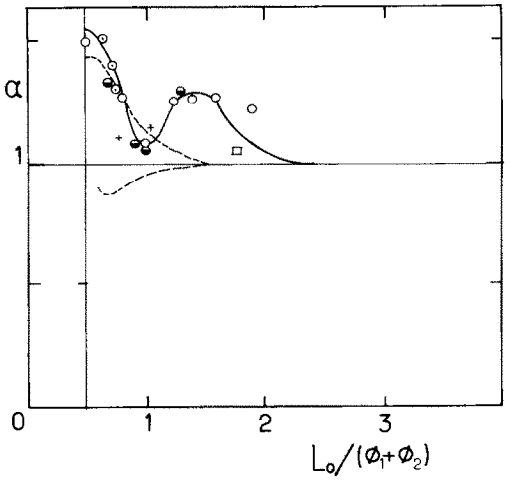

FIG. 2. Coupling coefficient vs axis gap spacing. ——, ref. [6].

$$C_x = 2(\Delta U_{\mathfrak{C}}/U_e)(L/\phi)\left[\int_{-\infty}^{\infty} f\,d\eta - (\Delta U_{\mathfrak{C}}/U_e) \times \int_{-\infty}^{\infty} f^2\,d\eta + \int_{-\infty}^{\infty} ((\overline{v'^2}-\overline{u'^2})/\Delta U_{\mathfrak{C}}^2)\,d\eta\right].$$

The order of magnitude of the turbulent term is about 1% of the other terms, so it can be neglected. The values of the integrals of f and f^2 according to equation (3) have been found equal to 1.995 and 1.475. So it is possible to write C_x in the following form:

$$C_x = 2(\Delta U_{\mathfrak{C}}/U_e)(L/\phi)[1.995-(\Delta U_{\mathfrak{C}}/U_e)1.475] \tag{9}$$

C_x being constant and equal to 1.15 in the range of the studied Reynolds number of 10^4, the product $(\Delta U_{\mathfrak{C}}/U_e)(L/\phi)$ is not really constant and the self preservation is only asymptotically reached. However, at the limit we can write

$$(\Delta U_{\mathfrak{C}}/U_e)(L/\phi) = 0.2882$$

while, from equations (4) we obtain that

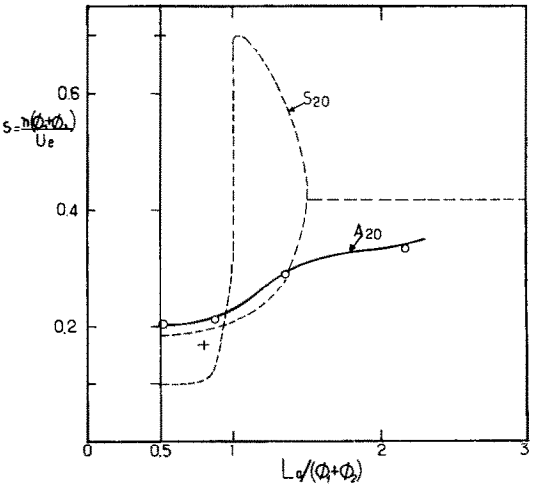

FIG. 3. Strouhal frequency. ——, ref. [6].

$$(\Delta U_{\mathrm{G}}/U_{\mathrm{e}})(L/\phi) = bc = 0.2909.$$

The difference, of only 1% between the two values, can be considered as acceptable as a first approximation.

2.2. *Double wake laws*

We consider now two parallel cylinders with ϕ_1 and ϕ_2 as respective diameters, with a length L_0 between the two axes, as shown on Fig. 1.

To define a self preservation zone in the double wake flow, we assume that L_0 is large enough so that the initial interaction between the two cylinders is small and $\alpha \simeq 1$. Then the effective drag of the couple can be taken equal to the sum of the two drags of each cylinder when considered alone.

To determine the mean dynamic field, we assume that in the third zone of the mixing, we can adopt a local hypothesis of linear interaction between the velocity of the two defects, that is

$$(\Delta\bar{u}/U_{\mathrm{e}}) = (\Delta U_{1\mathrm{M}}/U_{\mathrm{e}})f(\eta_1) + (\Delta U_{2\mathrm{M}}/U_{\mathrm{e}})f(\eta_2). \quad (10)$$

Then to study the mixing profile it is necessary to define the good physical frame for each wake. For that we define an asymmetry coefficient β as:

$$y_1 = y + \beta L_0$$
$$y_2 = y - (1-\beta)L_0.$$

From that definition and by considering equations (3) and (5), we obtain the following mean profile:

$$\begin{aligned}\Delta\bar{u}/U_{\mathrm{e}} = {} & (b/\sqrt{x})\{\sqrt{\phi_1}\exp -[(a/cx)(y+\beta L_0)^2/\phi_1] \\ & \times[(1+d)(y+\beta L_0)^4/(cx\phi_1)^2] \\ & + \sqrt{\phi_2}\exp -[(a/cx)\{(y-(1-\beta)L_0)^2/\phi_2\}] \\ & \times[1+\{d(y-(1-\beta)L_0)^4/(cx\phi_2)^2\}]\}. \quad (11)\end{aligned}$$

$y = 0$ is the location where the velocity defect becomes maximum. This condition is satisfied by taking

$$\beta = \sqrt{\phi_1}/(\sqrt{\phi_1}+\sqrt{\phi_2}) = \sqrt{\phi_1}/\sqrt{\tilde{\phi}} = r/(1+\sqrt{r})$$

with

$$r = \phi_1/\phi_2; \quad \tilde{\phi} = (\sqrt{\phi_1}+\sqrt{\phi_2})^2$$

and

$$\begin{aligned}(1-\beta) &= \sqrt{\phi_2}/(\sqrt{\phi_1}+\sqrt{\phi_2}) \\ &= \sqrt{\phi_2}/\sqrt{\tilde{\phi}} = 1/(1+\sqrt{r}). \quad (12)\end{aligned}$$

This maximum velocity defect will be noted as ΔU_{G}, following the relation

$$\Delta U_{\mathrm{G}}/U_{\mathrm{e}} =$$
$$(b/\sqrt{x^*})(\tilde{\phi}/L_0)\exp -\{(a/cx^*)[1+(d/(cx^*)^2)]\}. \quad (13)$$

In this expression we define the adimensional axis distance x^* as

$$x^* = x\tilde{\phi}/L_0^2 = x\phi_1/\beta^2 L_0^2 = x\phi_2/(1-\beta)^2 L_0^2. \quad (14)$$

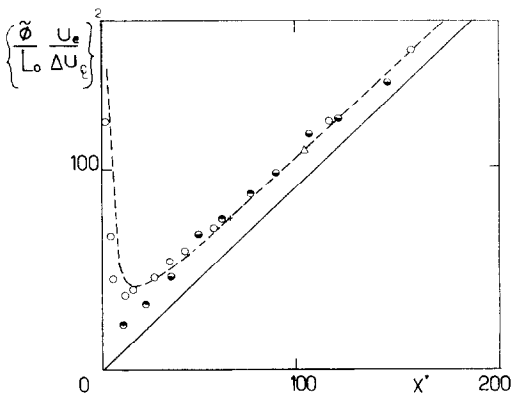

FIG. 4. Maximum velocity defect vs the downstream distance: ○, S_{20}, $r = 1$, $L_0 = 3/2(\phi_1+\phi_2)$; ◒, A_{20}, $r = 0.5$, $L_0 = (\phi_1+\phi_2)4/3$; △, A_{20}, $r = 0.6$, $L_0 = 0.687(\phi_1+\phi_2)$; +, A_{20}, ref. [10]; ——, $U_e/\Delta U_M^2 = (1/b^2)(x/\phi_1)$; – – – –, calculation (12).

So, by expressing the product $[(\Delta U_{\mathrm{G}}/U_{\mathrm{e}})(L_0/\tilde{\phi})]^{-2}$ vs x^*, we obtain a universal function plotted as a dashed line on Fig. 4. For high values of x^*, this function tends towards the single cylinder law, drawn as a full line on Fig. 4. The minimum of the function corresponds to $x^* = 2a/c$ for which the first and the second derivatives of the mean velocity profile with respect to $y^* = y/L_0$ are simultaneously equal to zero. The corresponding profile is a typical 'piston' velocity profile with a plateau at the maximum value. Such a profile has effectively been experimentally measured [13].

The asymptotic convergence towards the single wake law for large x^* values is relatively slow, as the convergence towards the self preservation zone. However, we can estimate that the beginning of this zone occurs after the section $x^* = 80$ corresponding to the beginning of a quasi linear expansion of the mixing.

Now, to calculate the width of the mixing $L^* = L/L_0$, we have to solve the equation

$$(\Delta\bar{u}/U_{\mathrm{e}}) = 1/2(\Delta U_{\mathrm{G}}/U_{\mathrm{e}}).$$

We then obtain the following equation:

$$[(L^*/\beta)+1]^2 - 1 = B \quad (15)$$

with

$$\begin{aligned}B = {} & [-(cx^*/a)\ln\{(1/\beta)(1/2-(1-\beta) \\ & \times\exp -[(a/cx^*)\{(L^*/(1-\beta)-1)^2-1\}] \\ & \times[1+d/(cx^*)^2\{(L^*/(1-\beta)-1)^4 \\ & +(L^*/(1-\beta)-1)^2(L^*/\beta+1)^2+(L^*/\beta+1)^4\}] \\ & \times[1+\{d/(cx^*)^2\}(L^*/\beta+1)^4 \\ & +(L^*/\beta+1)^2+1]^{-1}.\end{aligned}$$

To solve this equation, it is necessary to proceed by successive numerical iterations to obtain the two solutions L_1^* and L_2^*. Then we obtain $L^* = [(L_1^*)+(L_2^*)]/2$ as a function of x^* and r as it can be seen

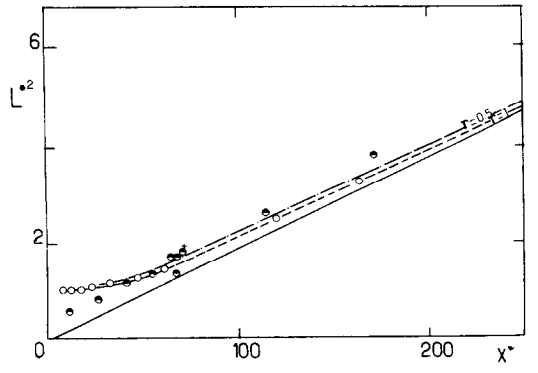

FIG. 5. Wake width laws: ○, S_{20}, $r = 1$, $L_0 = 3/2(\phi_1+\phi_2)$; ●, A_{20}, $r = 0.5$, $L_0 = (\phi_1+\phi_2)4/3$; +, A_{20}, ref. [10]; ——, $L^2 = 1/4(x\phi_1)$; – – –, present model.

on Fig. 5, on which, two curves of $L^*(x^*)$ are drawn as dashed lines, corresponding to $r = 1$ and 0.5. We can note that these two curves are not very different and asymptotically tend to the single cylinder law drawn as a full line for high values of x^*.

As previously noted, the convergence is slow, because of the exponential law. Also it is interesting to calculate an approximation of the linear law of $L^*(x^*)$ for high values of x^*.

For that we assume that $d = 0$ and choose $K' = Ka/C$ as the expansion coefficient, so that $L^* \approx Kx^*$. In that case, it is easy to show that K' obeys the equation

$$1/2 = \beta \exp -(K'/\beta^2)+(1-\beta)\exp -(K'/(1-\beta)^2) \tag{16}$$

which only depends on the variations of the asymmetry coefficient β.

This equation has no analytical solution but it can be approximated by $K' = \beta^2 \ln 2\beta$ for $\beta \approx 1$ and $K' = \beta^2 \ln 2$ for $\beta \approx 0.5$.

The exact solution is presented as a full line on Fig. 6 for the variations of $\beta(r)$ according to equations (12).

A more complete determination of K' shows that

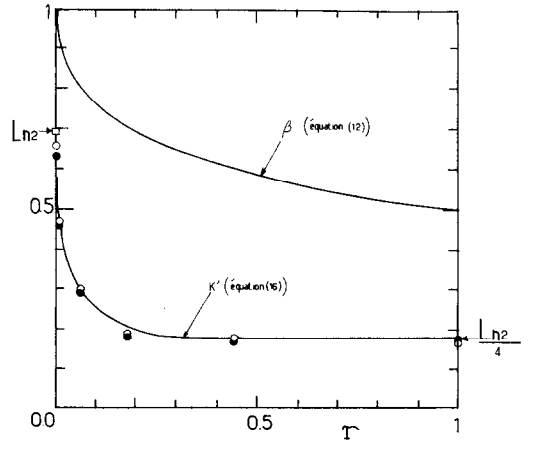

FIG. 6. Asymmetry parameter and expansion coefficient: ○, mixing of two wakes; ●, mixing of two jets.

$K'(r)$ weakly depends on the type of perturbation. So it is possible to extend the previous analysis to the mixing of two velocity excesses such as the mixing of two plane jets. With the definition of new constants for the plane jet expansion [15–17] it is possible to calculate the values of K' which are very close to those of the mixing of two cylinders plotted on Fig. 6.

It is also possible to introduce the coupling coefficient in the previous analysis and to realize the calculation for smaller gaps. However, new phenomena occur in this case, particularly the increasing of the vortex shedding effect behind the two cylinders which modifies the second mixing zone and the location where the self preservation zone begins.

On the other hand, to study the modifications of the single thermal wake by coupling another non-heated cylinder, we prefer to keep ϕ_1, U_e and $\Delta\Theta_0$ as the characteristic scales for the mean temperature field in the self preservation zone. The measuring section at $x^* = 72.2$ corresponds to the dynamic field at the end of the second mixing zone. It also corresponds to $x/\phi_1 = 46.2$ for the mean temperature field with the small heated cylinder. This section has been chosen to obtain a relatively good mixing and a sufficient overheat to measure temperature fluctuations with a good accuracy.

3. EXPERIMENTAL PROCEDURE

We performed measurements in air and water for Reynolds numbers of about 10^4. The cylinders used were built of brass. They were calibrated with a good constancy of the diameter all along the cylinder. Their surfaces were polished and lustred in order to get the same drag for cylinders with the same diameter and placed in the same flow conditions.

Four cases with different coupling coefficients have been studied and the geometrical and aerodynamical conditions are reported in Table 1.

Dynamically, the A_{21} case was identical to that of Palmer and Keffer [10] with a maximum shift between the zeros of the mean velocity gradient and the turbulent shear stress. The Reynolds number range is 2.5×10^3–1.7×10^4. The initial overheat $\Delta\Theta_0 = 7.7$ K.

In order to obtain a uniform heating for the cylinder in the air, a rolled up resistance was inserted in a quartz tube filled with sand. This quartz pipe was put in the brass tube and the resistance was electrically heated to obtain the studied temperature. However,

Table 1. Studied cases with initial conditions

	S_{11}	S_{20}	A_{20}	A_{21}
ϕ_1 (mm)	12	3	3	12
L_0 (mm)	0	9	9	22
ϕ_2 (mm)	0	3	6	20
$r = \phi_1/\phi_2$	∞	1	0.5	0.6
$\tilde{\phi}$ (mm)	12	12	17.68	62.98
$\Delta\Theta_0$ (K)	7.7	0	0	7.7
ϕ_1/H	0.015	0.015	0.004	0.015

it was necessary to get an absolute temperature of about 500 K on the brass cylinder surface to obtain $\Delta\Theta_0 = 7.7$ K. So, a change in cylinder diameter and gravity effects could occur in the boundary layer and radiative effects could occur between surfaces of the heated cylinder and the non-heated one. But with the velocity flow of 12 m s^{-1} we assumed that such effects were small enough and could be neglected.

The measurement techniques are the hot-wire anemothermometry, for the instantaneous velocity and temperature fields, and the thermocouple for the mean temperature. Different hot-wire probes were used: × wires and a three wire probe to measure simultaneously the fluctuating components of the velocity and of the temperature. The temperature fluctuations were obtained from a platinum wire of 1 μm diameter and 0.3 mm in length. It was compensated in the high frequency range and a constant current between 150 and 500 μA was used. It has been found that the best value for the current was about 350 μA to get a good signal/noise ratio and a weak velocity influence. However, the hot-wire signal was corrected for the temperature contamination using special electronic circuitry after the determination of the calibration curves [18]. So the fluctuations u', v' and θ' were recorded on a magnetic tape and a numerical treatment was realized to determine the double correlations and the frequency analysis.

Visualizations of the flow have been realized in similitude in a water channel of 20 × 20 cm square section, 1.20 m in length and a 17 cm s^{-1} flow velocity. The technique of dye emission has been used from needles placed upstream in the convergent section of the channel to see the emission lines in the potential flow, and from the rear of the cylinder, in the recirculating zone, to see the mixing wake. We also used LDA in the same water channel [9].

The information obtained by the two ways (hot-wire and visualization) is complementary and gives a better understanding of the different diffusive mechanisms.

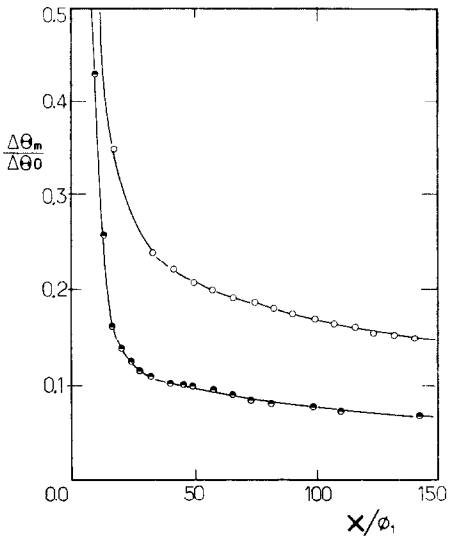

FIG. 7(a). Decrease of the temperature excess with the distance x/ϕ_1: ●, A_{21}; ○, S_{11}.

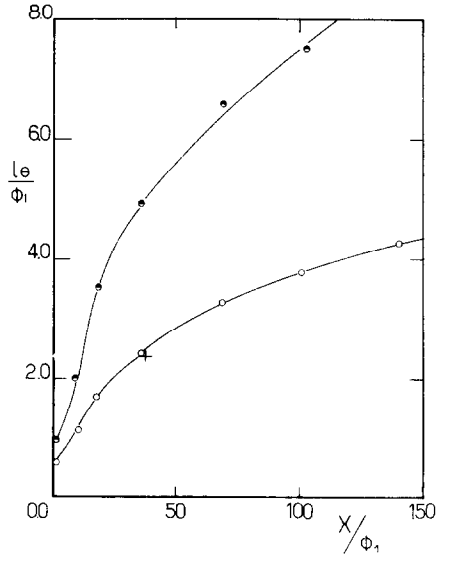

FIG. 7(b). Increase of the thermal wake width: ●, A_{21}; ○, S_{11}.

4. EXPERIMENTAL RESULTS

Firstly we present results concerning the mean dynamic and thermal fields, secondly results concerning the fluctuating fields in the (x, y) frame.

The single cylinder wake, the double mixing wakes, symmetrical and asymmetrical, are simultaneously studied by comparison. On Fig. 2 we have plotted the coupling coefficient α vs the gap spacing L_0 in the A_{20} and S_{20} cases. While two solutions occur for $L_0/(\phi_1+\phi_2) < 1.5$ in the S_{20} case, only one stable solution exists in the A_{20} case; and α increases up to 1.6 when the two cylinders are in contact. From the illustration shown on Fig. 14 the flow in the A_{20} case is shown to be constituted by a Bénard–von Kármán vortex street issued from the large cylinder, the other, downstream of the small cylinder, being almost completely destroyed. The curves of the Strouhal frequency, plotted on Fig. 3, vs $L_0/(\phi_1+\phi_2)$, show that in the asymmetrical case A_{20}, there is a single frequency for a given gap spacing which roughly corresponds to the lower solution for the S_{20} case.

On Figs. 4 and 5 the functions giving the maximum velocity defect in the double wake and the wake width vs the downstream distance x^* defined by equation (13) are drawn as dashed lines. The single wake laws are plotted as full lines. We note that a rather good prediction from the linear analysis is obtained; the prediction being better for a symmetrical case with a sufficient spacing gap $L_0/(\phi_1+\phi_2) > 1.5$, for which the coupling coefficient is close to 1. However, for the other cases, the behaviour is satisfactory after a certain distance downstream.

Figures 7(a) and (b) show the evolution of the

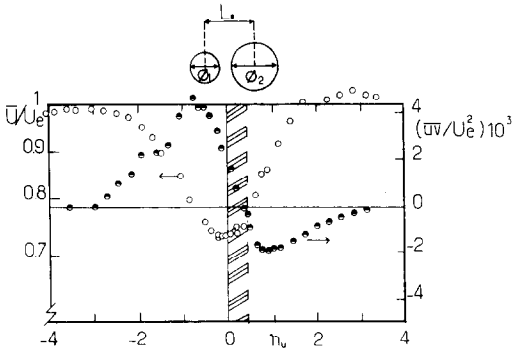

FIG. 8. Mean velocity and shear stress profiles (A_{20} case; $x^* = 72.2$).

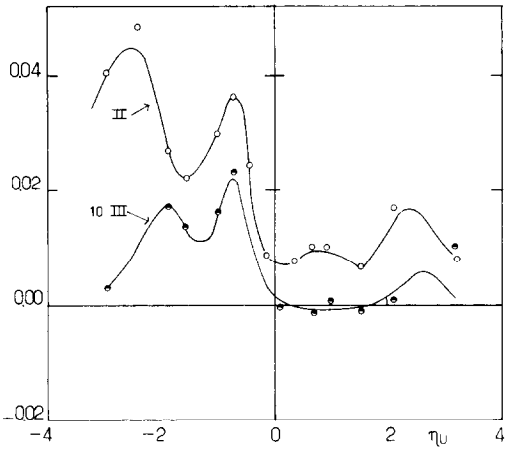

FIG. 10. Second and third invariants of the Reynolds stress tensor (A_{20} case; $x^* = 72.2$).

temperature excess and the thermal wake width as a function of the downstream distance x/ϕ_1. The data show that a strong increase of the thermal diffusion occurs in the asymmetrical double wake flow. The experiments were carried out in the geometrical configuration A_{21} (12, 22, 20). The thermal wake is more widely spread by a factor of 2 which can be interesting for applications. Principally this is due to the coherent structures of the flow generated behind the big cylinder. These eddies drive an important lateral flux which is quantifiable by considering the fluctuating field. So, in Fig. 8 the mean velocity profiles and the Reynolds stresses are drawn, at $x^* = 72.2$. A displacement between the zeros of the shear stress and of the velocity gradient, and then the presence of a counter-gradient diffusion zone can be noted. The turbulent intensity profiles of $\sqrt{(\overline{u'^2})}/U_e$; $\sqrt{(\overline{v'^2})}/U_e$; $\sqrt{(\overline{w'^2})}/U_e$ and $\sqrt{(\overline{q'^2})}/U_e$ are plotted on Fig. 9. It can be seen that these profiles exhibit two maxima, the higher one occurring behind the big cylinder. The profiles of the second and of the third stress tensor invariants are presented on Fig. 10

$$II = (\overline{u'_i u'_j}/\overline{q'^2})^2 - 1/3$$

$$III = [\overline{u'_i u'_j}^3/(\overline{q'^2})^3] - II - 1/9.$$

These invariants are small behind the big cylinder, showing consequently that the turbulence is not completely established on this side and that the kinetic energy of turbulence is not a good parameter to represent the turbulent state of the mixing. Here, the higher peak of $\sqrt{(\overline{q'^2})}$ is the consequence of the quasi periodic vortex shedding while only random fluctuations due to a turbulence level exist behind the small cylinder.

The diffusive effects of the large vortices can be seen on the mean temperature profile presented on Fig. 11. This profile exhibits two maxima corresponding, for the higher, to the longitudinal convection and, for the lower, to a lateral diffusion behind the large cylinder. So, in this asymmetrical case, the diffusive effects of the large eddies represent one of the most important features for this kind of flow.

Figure 12 shows the double correlation coefficients between u', v' and θ', and the intensities of the turbulent kinetic energy $\sqrt{(\overline{q'^2})}/U_e$ and the temperature variance $\sqrt{(\overline{\theta'^2})}/\Delta\Theta_M$. So, we can see also that a thermal counter-gradient diffusion zone occurs as well as a dynamical one, and that the two zones have a small common part between the relative minimum $\Delta\Theta_{min}$ and U_{min}. The correlation $Ru'\theta'$ always exhibits negative values corresponding to u' and θ' fluctuations with opposite sign. The curves of $\sqrt{(\overline{q'^2})}/U_e$ and $\sqrt{(\overline{\theta'^2})}/\Delta\Theta_M$ have two maxima not located on the same side of the wake. As noted before, this fact can

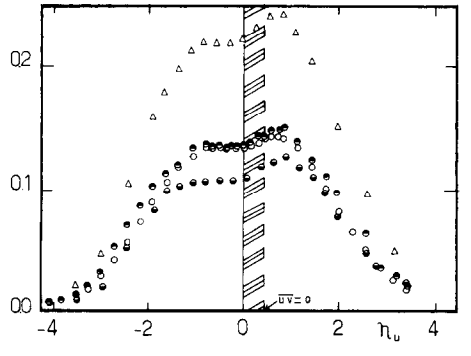

FIG. 9. Velocity components of turbulent intensities (A_{20} case; $x^* = 72.2$): ○, $\sqrt{(\overline{u'^2})}/U_e$; ●, $\sqrt{(\overline{v'^2})}/U_e$; ⊖, $\sqrt{(\overline{w'^2})}/U_e$; △, $\sqrt{(\overline{q'^2})}/U_e$.

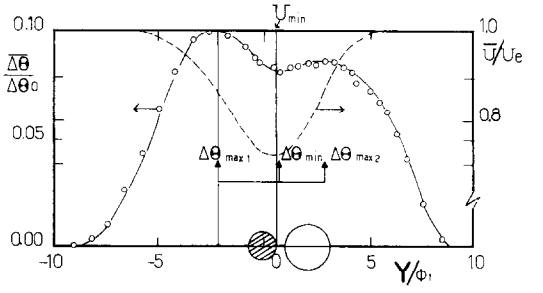

FIG. 11. Mean velocity and temperature profiles (A_{21} case; $x^* = 72.2$ or $x/\phi_1 = 46.16$).

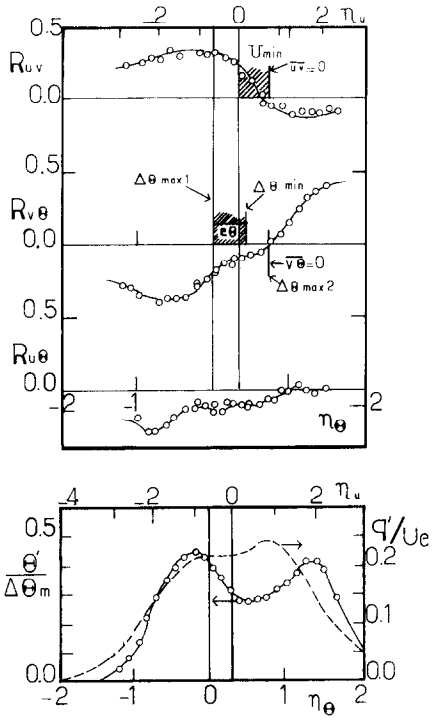

FIG. 12. Double correlation coefficients and turbulent intensities of the dynamical and thermal fields (A_{21} case; $x/\phi_1 = 46.16$; here θ' and q' denote the r.m.s. values).

FIG. 14. Scheme of the vortex shedding in the A_{21} case: shading, turbulent zone; —·—, centre-line; ⇝, counter-gradient diffusion.

be related to the different turbulent states on each side of U_{min}.

On Fig. 13 we present the dynamic and thermal turbulence productions at the studied section.

The reduced production π_u^* and π_θ^* are given by the expressions

$$\pi_u^* = -[\overline{u'v'}(\delta\bar{U}/\delta y) + (\overline{u'^2} - \overline{v'^2})(\delta\bar{U}/\delta x)](L/U_e^3)$$

$$\pi_\theta^* = -[\overline{v'\theta'}(\delta\bar{\theta}/\delta y) + \overline{u\theta}(\delta\bar{\theta}/\delta x)](L_\theta/U_e\Delta\Theta_{max}^2).$$

We only assume that the flow is two-dimensional in mean. As can be seen these two turbulent productions exhibit negative values in the corresponding counter-gradient diffusion zone. The negative values are more important for the thermal field than for the dynamic field and reach 14% of the maximum positive values of the production behind the small cylinder.

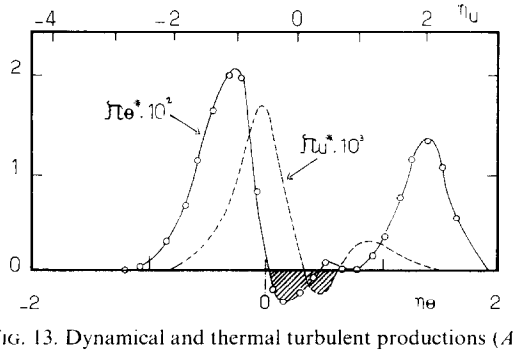

FIG. 13. Dynamical and thermal turbulent productions (A_{21} case; $x/\phi_1 = 46.16$).

Such results can be also found in various types of turbulent flows [19] or in free mixing shear flows [4].

The lateral heat flux responsible for this counter-gradient diffusion and to the negative turbulence production of the temperature variance, can be detected from flow visualization. A scheme of the diffusion is drawn on Fig. 14. This figure shows the two cylinders in the A_{20} case placed in a water channel. The temperature is replaced by dye emitted from a hypodermic needle placed in the recirculation zone of the small cylinder and diffusing in its wake. From this visualization we can see how the contaminant is diffused in the mixing of the two wakes, and we recognize the two diffusive mechanisms contributing to the spread of the dye. The first one is due to the relatively high level of turbulence existing just behind the small cylinder. The second comes from the vortex shedding, i.e. from the large eddies of the flow generated behind the large cylinder. These large eddies roll up, on their top, the fluid coming from the small cylinder wake. This capture contributes to the second maximum of the mean temperature profile in the heated case. This phenomenon is due to the interaction of the large eddies on the mean scalar field carrying along an important lateral heat flux, from the small to the large cylinder.

The asymmetrical configuration shown on Fig. 14 also exists in the double wake flow of two cylinders of the same diameter with a small gap [9] but it randomly oscillates between two positions with the vortex street on the left or on the right while it remains on one side in the present asymmetrical case with the vortex street

situated behind the large cylinder. On this point of view the asymmetrical vortex shedding is a more stable fluidic dynamical system.

5. CONCLUSIONS

From the experimental study of the asymmetrical dual wake with heat transfer, several results have been obtained. At first, for the mean dynamic field, it is possible to predict the variations of the maximum velocity defect and of the wake width, from the single wake laws, assuming a linear hypothesis. We conclude that a zone of quasi similitude can be obtained downstream, beyond $\tilde{\phi}x/L_0^2 > 80$ with $\tilde{\phi}$ an equivalent diameter taking into account the initial geometry of the cylinder twin. Below a certain gap between the two cylinders, there are specific discrepancies between the symmetrical and the asymmetrical double wake flows. While the flow is oscillating between two solutions in the first case, the flow is relatively stable in the second case with only one vortex street behind the big cylinder. In this asymmetrical dual wake the vortex street behind the small cylinder is almost completely destroyed and a rapid and large turbulent diffusion occurs. So a pollutant, or the heat coming from the surface of the small cylinder is more rapidly spread by a factor of two. It is then possible to detect countergradient diffusions and negative values for the dynamic and thermal productions of turbulence. This phenomenon can be related to a predominant lateral flux generated by the large eddies of the flow issued from the big cylinder. These eddies carrying along on their top the wake of the small cylinder, induce an important lateral flux and consequently a typical mean temperature profile with two maxima, one being due to the longitudinal advection and the other to this lateral flux. Visualizations of the flow confirm these explanations. From the asymmetry of the dual wake with a high level of turbulence behind the small cylinder and a vortex street behind the large cylinder, it is possible then to find again the sign of the countergradient diffusion as a function of the real turbulent intensity gradient [4].

REFERENCES

1. S. Eskinazi and F. F. Erian, Energy reversal in turbulent flows, *Physics Fluids* **12**, 1968–1988 (1969).
2. A. F. Kurbatski and N. N. Yanenko, On the modelling of effects of negative production of temperature fluctuation intensity in the turbulent mixing layer, *J. Fluid Mech.* **130**, 453–462 (1983).
3. C. Béguier, Mesures des tensions de Reynolds dans un écoulement dissymétrique en régime turbulent incompressible, *J. Méc. Théorique Appliquée* **4**, 319–329 (1965).
4. C. Béguier, L. Fulachier and J. F. Keffer, The turbulent mixing layer with an asymmetrical distribution of temperature, *J. Fluid Mech.* **89**, 561–587 (1978).
5. M. M. Zdravkovich, Review of flow interference between two circular cylinders in various arrangements, *ASME J. Fluid Engng* **99**, 618–633 (1977).
6. P. W. Bearman and A. J. Wadcock, The interaction between a pair of circular cylinders normal to a stream, *J. Fluid Mech.* **61**(3), 499–511 (1973).
7. L. Landweber, Flow about a pair of adjacent, parallel cylinders normal to a stream, David Taylor Model Basin, Report No. 485, Navy Department, Washington (1942).
8. H. M. Spivack, Vortex frequency of flow pattern in the wake of two parallel cylinders at varied spacing normal to an air stream, *J. Aero. Sci.* **13**(6), 289–301 (1946).
9. C. Domptail, Sillage turbulent en aval de deux barreaux parallèles en tunnel hydrodynamique: visualisation et vélocimétrie laser, Thèse de 3ème Cycle, Université d'Aix-Marseille II (1979).
10. M. D. Palmer and J. F. Keffer, An experimental investigation of an asymmetrical turbulent wake, *J. Fluid Mech.* **53**, 593–610 (1972).
11. A. A. Townsend, *The Structure of Turbulent Shear Flow*. Cambridge University Press, London (1956).
12. C. C. Alexopoulos and J. F. Keffer, Extended measurements of the two-dimensional turbulent wake, Dept. Mech. Engng, Univ. of Toronto, U.T. Mech, ETP 6811 (1968).
13. P. Fraunié, Contribution à l'étude des champs dynamique et thermique dans le sillage de deux cylindres de section circulaire, Thèse de Docteur-Ingénieur, Université d'Aix-Marseille II (1979).
14. A. E. Davies, J. F. Keffer and D. W. Baines, Spread of a heated plane turbulent jet, *Physics Fluids* **18**(7), 770–775 (1975).
15. C. Béguier, Etude du jet plan dissymétrique en régime turbulent incompressible, Thèse d'Etat, Université d'Aix-Marseille II (1971).
16. E. Förthmann, Turbulent jet expansion, Tech. Memo NACA No. 789, Vol. 5, No. 1 (1936).
17. L. S. J. Bradbury, The structure of a self-preserving turbulent plane jet, *J. Fluid Mech.* **23**(1), 31–64 (1965).
18. R. Mangouala, Contribution à l'étude du champ thermique en aval de deux cylindres de diamètres différents, Thèse de 3éme Cycle, Université d'Aix-Marseille II (1981).
19. I. Wygnanski, D. Oster and H. Fiedler, *A Forced Plane Turbulent Mixing Layer: a Challenge for the Predictor*, pp. 314–326. Springer, Berlin (1979).

SILLAGE DOUBLE AVEC TRANSFERT DE CHALEUR

Résumé—L'étude présentée concerne l'évolution des champs dynamique et thermique en aval d'un couple de cylindres. Différentes configurations ont été étudiées avec des cylindres de diamètres identiques ou différents, l'un étant chauffé ou non et l'entraxe étant variable. Une étude des paramètres de similitude du champ dynamique a d'abord été réalisée à partir des lois du sillage simple, en supposant l'interaction initiale faible et la linéarisation du problème. A partir de la définition d'un diamètre équivalent et d'un paramètre de dissymétrie, on a pu déterminer les lois de décroissance du créneau maximum de vitesses ainsi que l'évolution de la largeur de brassage du mélange en fonction de la distance aval. Les résultats obtenus peuvent être généralisés au cas de deux perturbations planes et en particulier au cas du mélange de deux jets plans en écoulement uniforme. La partie expérimentale de cette étude présente des mesures au fil chaud et des visualisations en tunnel hydrodynamique. Les résultats du champ dynamique moyen sont en bon accord avec les calculs précédents de la zone de similitude. Les mesures du champ turbulent, en particulier des corrélations doubles et triples entre les fluctuations de vitesse et de température, montrent l'existence de flux à contre-gradient dynamique et thermique dans le cas du couple de cylindres de diamètres différents et à faible entr'axe. Ces flux peuvent être reliés aux grosses structures tourbillonnaires créant une diffusion latérale importante du petit vers le gros barreau.

ZWEIFACHE WIRBELSCHLEPPE MIT WÄRMEÜBERTRAGUNG

Zusammenfassung—In dieser Arbeit werden die Geschwindigkeits- und Temperaturfelder im Nachlauf eines umströmten Zylinderpaares behandelt. Unterschiedliche Anordnungen werden untersucht: Die Zylinder besitzen gleichen oder unterschiedlichen Durchmesser, einer der Zylinder ist beheizt oder auch nicht, der Abstand ist variabel. Zuerst werden aus den Gesetzmäßigkeiten für den Einzelzylinder die Ähnlichkeitskennzahlen für die zweifache Wirbelschleppe bestimmt, wobei angenommen wird, daß die anfängliche Wechselwirkung schwach und das Problem linearisierbar ist. Es wird ein äquivalenter Durchmesser und ein Koeffizient für die Asymmetrie definiert. Damit ist es möglich, die Fortpflanzung des Geschwindigkeitsdefekts und die Breite des vermischenden Nachlaufs zu berechnen. Die analytische Betrachtung kann auf die Vermischung zweier ebener Störungen, wie z. B. die Vermischung zweier ebener Strahlen, in einer gleichförmigen Strömung ausgedehnt werden. Im experimentellen Teil der Untersuchung werden Ergebnisse von Hitzdrahtmessungen sowie die Sichtbarmachung der Vorgänge in einem hydrodynamischen Strömungskanal vorgestellt. Die Ergebnisse für das Feld der mittleren Geschwindigkeit stimmen recht gut mit theoretischen Berechnungen im Ähnlichkeitsgebiet überein. Die Messungen bei turbulenter Strömung zeigen bei zweifacher und dreifacher Korrelation zwischen den Geschwindigkeits- und Temperaturschwankungen für den asymmetrischen Fall die Existenz von Diffusionsvorgängen entgegen dem Gradienten. Diese Ströme können auf die größten Wirbel in der Strömung zurückgeführt werden, die einen wesentlichen Beitrag zur seitlichen Diffusion vom kleinen zum großen Zylinder leisten.

ТЕЧЕНИЕ С ДВОЙНЫМ СЛЕДОМ ПРИ ТЕПЛОПЕРЕНОСЕ

Аннотация—Исследуются динамические и тепловые поля вниз по течению от пары цилиндров. Рассматриваются различные конфигурации: цилиндры с одинаковыми или различными диаметрами, один из которых нагрет или не нагрет, а исходный зазор изменяется. Сначала по законам следа за единичным цилиндром определяются критерии подобия течения с двойным следом в предположении слабого начального взаимодействия и линеаризации задачи. Из определения эквивалентного диаметра и коэффициента асимметрии можно рассчитать эволюции максимального дефекта скорости и ширину смешения следов. Представленный анализ может быть распространен на случай смешения двух двумерных возмущений, таких как смешение двух плоских струй в равномерном потоке. Затем в экспериментальной части исследования приводятся данные измерений термоанемометрическим методом и визуализации в гидродинамической трубе. Данные по среднему динамическому полю весьма удовлетворительно согласуются с теоретическими результатами в автомодельной области. Измерения в турбулентном поле двойных и тройных корреляций между пульсациями скорости и температуры показывают наличие в асимметричном случае противоградиентных диффузионных потоков. Эти потоки могут быть связаны с максимальными вихрями течения, создающими существенную поперечную диффузию от малого цилиндра к большому.